NASA Contractor Report 178270

ICASE REPORT NO. 87-19

ICASE

ACOUSTIC GRAVITY WAVES: A COMPUTATIONAL APPROACH

S. I. Hariharan

P. K. Dutt

INSTITUTE FOR COMPUTER APPLICATIONS IN SCIENCE AND ENGINEERING
NASA Langley Research Center, Hampton, Virginia 23665

Operated by the Universities Space Research Association

NASA

National Aeronautics and
Space Administration

Langley Research Center
Hampton, Virginia 23665

Acoustic Gravity Waves: A Computational Approach

S.I.Hariharan

Department of Mathematical Sciences
University of Akron, Akron, OH 44325
and
Institute for Computer Applications in Science and Engineering

P.K.Dutt

Institute for Computer Applications in Science and Engineering
NASA, Langley Research Center, Hampton, VA 23665

ABSTRACT

This paper discusses numerical solutions of a hyperbolic initial boundary value problem that arises from acoustic wave propagation in the atmosphere. Field equations are derived from the atmospheric fluid flow governed by the Euler equations. The resulting original problem is nonlinear. A first order linearized version of the problem is used for computational purposes. The main difficulty in the problem as with any open boundary problem is in obtaining stable boundary conditions. Approximate boundary conditions are derived and shown to be stable. Numerical results are presented to verify the effectiveness of these boundary conditions.

Acoustic Gravity Waves: A Computational Approach

S.I.Hariharan

Department of Mathematical Sciences
University of Akron, Akron, OH 44325
and
Institute for Computer Applications in Science and Engineering

P.K.Dutt

Institute for Computer Applications in Science and Engineering
NASA, Langley Research Center, Hampton, VA 23665

1. Introduction

In this paper we present results concerning a model problem that arises in the study of nonlinear acoustic wave propagation in the atmosphere. The derivation follows after Cole & Greifinger [1], and the details are presented in the appendix. In an earlier study Hariharan [3,4] discussed a strictly two dimensional version of this problem. In these references the well-posedness of the problem was discussed, and results concerning stable boundary conditions were presented. The present paper discusses an axisymmetric three dimensional model. It is well known that the nature of wave propagation varies drastically between two and three dimensions and two dimensional results are not special cases of the three dimensional results. To this end the present study is motivated by possible comparisons with future experimental results. Needless to say the experiments will be three dimensional, and any comparable theoretical model also has to be in three dimensions. Most of the acoustic wave propagation experiments are done in a laboratory environment; therefore, simulation of actual nonlinear effects is rather difficult. In particular, long range wave propagation in the atmosphere is a difficult situation to simulate in the laboratory. As a result we shall confine ourselves to obtaining numerical results for only a linear version of the problem, which is a difficult problem in itself. Moreover, a careful study of this problem will lead to meaningful nonlinear corrections later once we have some experimental results.

In [2], it was pointed out that the nonlinear problem can be solved by obtaining a sequence of linear problems successively. Each succeeding problem contains the solution of the previous problem as forcing terms. It was also proved in [2] that the problems were well-posed. We develop analogous arguments for the axisymmetric three dimensional case in this paper. However, our main focus here is to obtain numerical solutions for the first linear problem that arises in the present study.

Let us present the problem (see appendix) under consideration. The model assumes the following situation as explained in the appendix.

(i)   Ground (earth) is flat.

(ii)   Atmosphere is isothermal.

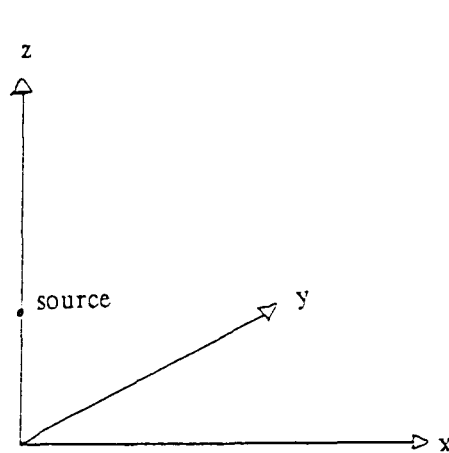(iii) Pressure and density vary exponentially (standard model).

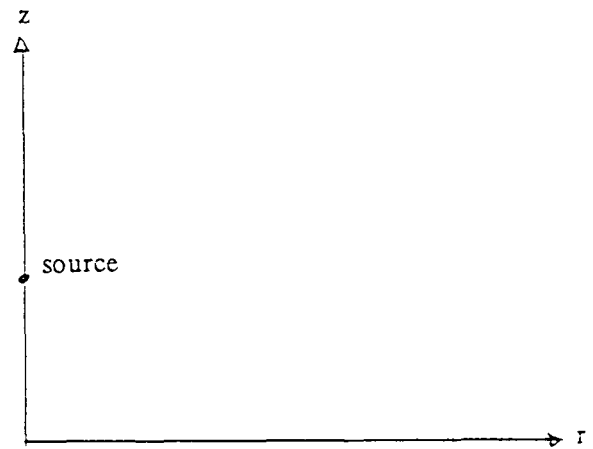Figure (1.1 a)   Figure (1.1 b)

The problem is posed on a half space $(-\infty,\infty)\times(-\infty,\infty)\times[0,\infty)$ with a point source (figure 1.1 a) at z_0 emitting acoustic waves. Due to axisymmetry, we consider the problem in the quarter space $[0,\infty)\times[0,\infty)$ (in polar coordinates). If $\rho,u,v,$ and p denote the acoustic density, acoustic velocity components in the r and z directions and acoustic pressure respectively, then the governing equations are:

$$\rho_t + u_r + \frac{u}{r} + w_z - w = 0 \qquad (1.1)$$

$$u_t + \frac{1}{\gamma}p_r = 0 \qquad (1.2)$$

$$w_t + \frac{1}{\gamma}p_z - \frac{(p-\rho)}{\gamma} = 0 \qquad (1.3)$$

$$p_t + \gamma u_r + \gamma w_z + \gamma\frac{u}{r} - w = f(r,z,t) \qquad (1.4)$$

where $\gamma = 1.4$, $f(r,z,t)$ describes the nature of the acoustic source and $r = \sqrt{x^2+y^2}$.

Boundary Conditions are:

$$w(r,0,t) = 0, \quad t > 0 \qquad (1.5)$$

$$u(r,z,t)/r \text{ is bounded as } r\rightarrow 0. \qquad (1.6)$$

Initial Conditions are:

$$p = \rho = u = w = 0 \text{ for } t = 0. \qquad (1.7)$$

For convenience, we shall call the initial boundary value problem defined through (1.1) - (1.7) problem (P). As mentioned earlier, problem (P) is the first linearized problem that results from the acoustic equations. Our goal is to solve (P) numerically. As in any open boundary problems, the problem at hand cannot be solved numerically unless the infinite region is truncated to a finite one. When we do such a truncation, we also have to provide boundary conditions on these truncated boundaries. They have to simulate the behavior at infinity and should be absorbing boundary conditions. Moreover the problem in the truncated region must be well-posed. Thus the plan of the paper is as follows: First we construct radiation boundary conditions that simulate the behavior at infinity at finite distances. Then we show that the problem in the truncated region is well-posed. Then we present the numerical technique along with some numerical boundary conditions that are required to stabilize the numerical scheme. Finally, we present some examples to validate the numerical scheme and to interpret the physics behind the problem.

2. Absorbing boundary conditions

As mentioned earlier, it is essential to truncate the boundaries that are at infinity to the ones at finite distances. Thus we do the truncation into a finite region $[0,L] \times [0,H] \equiv \Omega$. The situation is shown in figure 2.1.
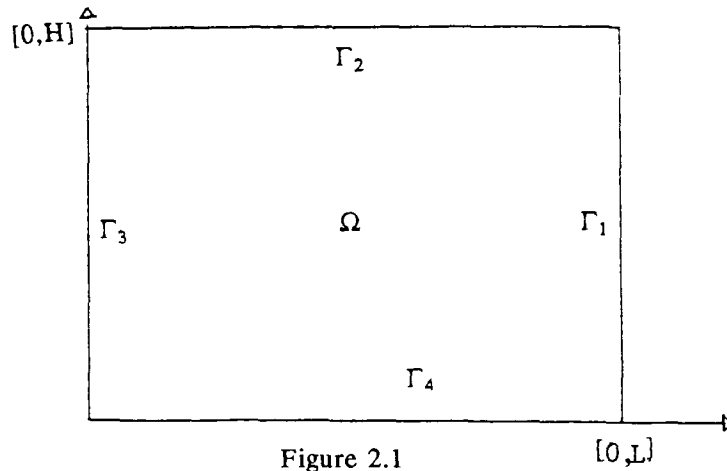
Figure 2.1

To obtain radiative or absorbing boundary conditions, there are a variety of procedures. One way to construct such boundary conditions is to obtain appropriate inflow and outflow variables for the system. This procedure is similar to obtaining appropriate Riemann invariants. For successful implementations in one dimension see Hariharan and Lester[4]. However, the problem under consideration is a quasi two-dimensional problem. An exact construction of the Riemann invariant is not possible. But an acceptable procedure which is approximate is to consider one-way wave equations in the r and z directions and obtain the Riemann invariants. To do this let us note that the system of equations under consideration (equations (1.1)-(1.4)) can be written in the form:

$$\mathbf{u}_t + \mathbf{A}\mathbf{u}_r + \mathbf{B}\mathbf{u}_z + \mathbf{C}\mathbf{u} = \mathbf{F} \tag{2.1}$$

where,

$$\mathbf{A} = \begin{bmatrix} 0 & 1 & 0 & 0 \\ 0 & 0 & 0 & \dfrac{1}{\gamma} \\ 0 & 0 & 0 & 0 \\ 0 & \gamma & 0 & 0 \end{bmatrix}$$

$$\mathbf{B} = \begin{bmatrix} 0 & 0 & 1 & 0 \\ 0 & 0 & 0 & 0 \\ 0 & 0 & 0 & \dfrac{1}{\gamma} \\ 0 & 0 & \gamma & 0 \end{bmatrix}$$

$$\mathbf{C} = \begin{bmatrix} 0 & \dfrac{1}{r} & -1 & 0 \\ 0 & 0 & 0 & 0 \\ \dfrac{1}{\gamma} & 0 & 0 & -\dfrac{1}{\gamma} \\ 0 & \dfrac{\gamma}{r} & -1 & 0 \end{bmatrix}$$

$$\mathbf{F} = [0,0,0,f]^T \quad \text{and} \quad \mathbf{u} = [\rho,u,w,p]^T.$$

At large distances the effect of the source term vanishes. Thus the <u>one</u> <u>way</u> wave equation in the r

direction is

$$\mathbf{u}_t + \mathbf{A}\mathbf{u}_r = 0 \tag{2.2}$$

and in the z direction it is

$$\mathbf{u}_t + \mathbf{B}\mathbf{u}_z = 0. \tag{2.3}$$

We note that we have neglected the lower order terms in this process, and this again is an acceptable procedure to obtain boundary conditions. The final step is to diagonalize the matrices $\mathbf{A}$ and $\mathbf{B}$ through a change of variable $\mathbf{u}$ of the form $\mathbf{u} = \mathbf{T}\mathbf{v}$, so that $\mathbf{T}^{-1}\mathbf{A}\mathbf{T}$ and $\mathbf{T}^{-1}\mathbf{B}\mathbf{T}$ are diagonal. The elements of the resulting diagonal matrices will contain the eigenvalues of $\mathbf{A}$ and $\mathbf{B}$. The matrix $\mathbf{T}$ in each case is constructed using the eigenvectors of $\mathbf{A}$ and $\mathbf{B}$. This leads to the construction of the inflow and outflow variables at the boundaries Γ_1 and Γ_2 (figure 2.1). The inflow variables on these boundaries are $p - \gamma u$ on Γ_1 and $p - \gamma w$ on Γ_2. Thus for radiating boundaries we require that these variables be zero and obtain the radiation boundary conditions. They are

$$p - \gamma u = 0 \quad \text{on } \Gamma_1 \tag{2.4}$$

and

$$p - \gamma w = 0 \quad \text{on } \Gamma_2. \tag{2.5}$$

In the next section we shall show that the problem (P) together with boundary conditions (2.4) and (2.5) yield a well-posed problem.

One should note that these boundary conditions are the lowest order boundary conditions, and as such one has to keep the truncated boundaries Γ_1 and Γ_2 at far distances to obtain minimal reflections from infinity. To obtain higher order boundary conditions, one has to resort to a different strategy. One needs to obtain the dispersion relations of the problem under consideration. These dispersion relations can also be interpreted in the pseudo differential operator terminology. Whatever the case may be, the ideas lead to obtaining boundary operators that dictate radiativity. For associated details we refer readers to [5,6]. In these references only simple wave equations or problems that are not of the characteristic type are discussed. The current problem as we will see has a complicated structure. To investigate further, let us consider the governing equations of (P). Suppose we are interested in obtaining radiation conditions on the boundary Γ_1. We take the Laplace transform in time of equations (1.1)-(1.4) to

obtain:

$$s\overline{p} + \overline{u}_r + \frac{\overline{u}}{r} + \overline{w}_z - \overline{w} = 0 \tag{2.7}$$

$$s\overline{u} + \frac{1}{\gamma}\overline{p}_r = 0 \tag{2.8}$$

$$s\overline{w} + \frac{1}{\gamma}\overline{p}_z - \frac{(\overline{p} - \overline{p})}{\gamma} = 0 \tag{2.9}$$

$$s\overline{p} + \gamma\overline{u}_r + \gamma\overline{w}_z + \gamma\frac{\overline{u}}{r} - \overline{w} = 0. \tag{2.10}$$

Here for any function $h(r,z,t)$ the Laplace transform is defined by

$$\overline{h}(r,z,s) = \int_0^\infty e^{-st}h(r,z,t) \, dt \tag{2.11}$$

which will be inverted according to

$$h(r,z,t) = \frac{1}{2\pi i} \int_{-i\infty}^{i\infty} e^{st}\overline{h}(r,z,s) \, ds. \tag{2.12}$$

Since our goal is to obtain radiating boundary conditions on Γ_2, i.e., in the z direction, we will transform the r variable also to obtain a system of ordinary differential equations in the z direction. Due to the presence of cylindrical symmetry, it is natural to use the Hankel transforms. For any function $g(r)$, the Hankel transform and its inverse are defined respectively by

$$\hat{g}(\omega) = \int_0^\infty g(r)J_\gamma(\omega r)r \, dr \qquad (\gamma > -\frac{1}{2}) \tag{2.13}$$

$$g(r) = \int_0^\infty \hat{g}(\omega)J_\gamma(\omega r)\omega \, d\omega \qquad (\gamma > -\frac{1}{2}). \tag{2.14}$$

Let

$$(\hat{\rho},\hat{w},\hat{p})(z;\omega,s) = \int_0^\infty (\overline{\rho},\overline{w},\overline{p})(z,r,s) \, J_0(\omega r)r \, dr \tag{2.15}$$

and

$$\hat{u}(z;\omega,s) = \int_0^\infty \overline{u}(z,r,s) \, J_1(\omega r)r \, dr. \tag{2.16}$$

With these definitions we apply the Hankel transforms to equations (2.7)-(2.10). We note that the definition of the transform is different for $\overline{u}$ than the other dependent variable. This is due to the singularity in r. However, the recurrence relations of the Bessel functions J_0 and J_1 account for the singularity and the final transformations look as if we took the Fourier transform ignoring the singular terms. We shall show the computations to one equation.

Multiplying equation (2.7) by $J_0(\omega r)r$ and integrating over r on the interval $[0,\infty)$, we get

$$s\hat{p} + \int_0^\infty (\bar{u}_r + \frac{\bar{u}}{r}) J_0(\omega r)r \, dr + \hat{w}_z - \hat{w} = 0.$$

We rearrange the integral term and integrate by parts to get

$$\int_0^\infty (r\bar{u})_r J_0(\omega r) \, dr = -\int_0^\infty \bar{u}[J_0(\omega r)]'r \, dr. \qquad (2.17)$$

The recurrence relation needed here is

$$[J_0(\omega r)]' = -\omega J_1(\omega r).$$

Thus the right hand side of (2.17) becomes $\omega \hat{u}$. Similar calculations applied to the remaining equations yield the following system of ordinary differential equations in z:

$$s\hat{p} + \omega \hat{u} + \hat{w}_z - \hat{w} = 0 \qquad (2.18)$$

$$s\hat{u} + \frac{\omega}{\gamma}\hat{p} = 0 \qquad (2.19)$$

$$s\hat{w} + \frac{1}{\gamma}\hat{p}_z - \frac{(\hat{p}-\hat{\rho})}{\gamma} = 0 \qquad (2.20)$$

$$s\hat{p} + \gamma \omega \hat{u} + \gamma \hat{w}_z - \hat{w} = 0. \qquad (2.21)$$

Seeking solutions of the form $e^{\lambda z}$, one obtains the following characteristic relations for the above system:

$$\lambda = \frac{1}{2} \pm \mu(s,\omega), \qquad (2.22)$$

where,

$$\mu(s,\omega) = \left[\frac{1}{4} + s^2 + \omega^2 + \beta^2 \omega^2/s^2\right]^{\frac{1}{2}}, \qquad (2.23)$$

and where,

$$\beta^2 = (\gamma-1)/\gamma^2 \quad (> 0).$$

This relation is the same as the dispersion relation for the strictly two dimensional model. It was argued in [2] that for propagation the ratio $\frac{\omega}{s}$ must be smaller than one, and the outgoing waves are given by (2.22) with the '-' sign. These lead to the observation that the dispersion relation

$$\lambda = \frac{1}{2} - \mu(s,\omega) \qquad (2.24)$$

can be approximated for large s and the approximations arising from (2.23) are found in [2]. The first

two approximations are

$$\lambda \approx \frac{1}{2} - s \tag{2.25}$$

$$\lambda \approx \frac{1}{2} - s - \frac{1}{8s} - \frac{\omega^2}{s}. \tag{2.26}$$

To obtain the absorbing boundary operators, we multiply (2.25) by $e^{\lambda z}$ and an appropriate dependent variable, in this case the acoustic pressure. This leads to the differential operator (approximate) in the transform domain

$$\hat{p}_z = \frac{1}{2}\hat{p} - s\hat{p}. \tag{2.27}$$

Now we apply the inversion formulas (2.12) and (2.14) to get the required approximate boundary condition

$$p_z = \frac{1}{2}p - p_t. \tag{2.28}$$

For the second approximation (2.26), to carry out this procedure one must multiply the equation by s. This requirement is easily seen from the equation because it contains s in the denominator, which causes difficulties in the inversion. Then the rest of the procedure holds, and the resulting boundary operator is

$$p_{zt} = \frac{1}{2}p_t - p_{tt} - \frac{p}{8} - \frac{1}{2}p_{rr}. \tag{2.29}$$

A similar procedure can be used to derive boundary conditions on the boundary Γ_1. However, from (2.29) one must note that the boundary condition is second order, while the system we want to solve is first order. This leads to an undesirable situation for numerical implementations. Also, we have not proved that (2.28) or (2.29) are stable boundary conditions, i.e., they yield a well-posed problem in the sense of an energy estimate discussed in the next section. However, the above higher order boundary conditions are possible candidates to explore computational efficiency.

It is interesting to note that in equation (2.28) if we neglect the lower order term we obtain a further approximation in the form:

$$p_z = -p_t. \tag{2.30}$$

Moreover, if we incorporate equation (1.3) neglecting the lower order terms, equation (2.30) becomes

$$p_t - \gamma w_t = 0. \tag{2.31}$$

Integrating (2.31) using the initial conditions, one obtains the approximate boundary condition

$$p - \gamma w = 0 \quad (\text{on } \Gamma_2) \tag{2.32}$$

which is the same as (2.4) which we obtained through the characteristics. For this reason we shall refer to (2.32) as the zeroth order boundary condition and (2.28) as the first order boundary condition. Our discussion and numerical experiments on the problem pertains only to the zeroth order condition. There are two reasons for such a consideration. First is the difficulty in establishing well-posedness of the problem with the higher order boundary conditions. The second one is due to the fact that it is desirable to establish a solution procedure with a simpler set of boundary conditions, which has the theoretical backing rather than concern ourselves about the accuracy and computational efficiency with higher order conditions, for which we do not have the analysis yet.

3. Energy Estimates

Here, we show that the problem (P) together with the absorbing boundary conditions (2.32) lead to a well-posed problem. To do so we consider an appropriate energy for the problem in the truncated region Ω and show it is bounded by the energy supplied through the source. Recall that the governing equations can be written in the form (equation (2.1))

$$u_t + A u_r + B u_z + C u = 0. \tag{3.1}$$

Also, physical considerations yield the boundary conditions on Γ_3 and on Γ_4 (see figure 2.1)

$$u |_{\Gamma_3} = 0 \quad (\text{on the axis}) \tag{3.2}$$

and

$$w |_{\Gamma_4} = 0 \quad (\text{on the ground}). \tag{3.3}$$

Radiation conditions are

$$(p - \gamma u) |_{\Gamma_1} = 0 \tag{3.4}$$

$$(p - \gamma w) |_{\Gamma_2} = 0. \tag{3.5}$$

The definition of the vectors u, F, and the matrices A, B, and C are as in section 2. Also we have the initial condition

$$\mathbf{u} = 0 \quad (t=0). \tag{3.6}$$

We call the problem defined through (3.1) - (3.6) (P'). We show here the following:

Theorem 3.1

Problem (P') is well-posed satisfying an energy estimate of the form

$$\int_0^T \|e^{-\eta t}\mathbf{u}\|_0^2 \, dt \leq C\eta^{-1}\int_0^T \|e^{-\eta t}\mathbf{F}\|_0^2 \, dt, \tag{3.7}$$

where the norm $\|.\|_0$ is the L_2 norm in Ω, C is a constant independent of $\mathbf{F}$, for all $\eta > K$, a positive constant.

To prove this theorem we note that the system (3.1) is a system of hyperbolic partial differential equations, but it is not strictly hyperbolic. As such Kreiss's stability theory [7] for the given initial boundary value problem is not directly applicable. However, we obtain energy estimates as in theorem 3.1. To do that we need a matrix G such that the matrices $\mathbf{M} = \mathbf{GAG}^{-1}$ and $\mathbf{N} = \mathbf{GBG}^{-1}$ are symmetric. If we multiply equation (3.1) on the left by the matrix $\mathbf{S} = \mathbf{GG}^T$, then it takes the form

$$\mathbf{Su_t + Pu_r + Qu_z + SCu = SF} \tag{3.8}$$

where $\mathbf{P} = \mathbf{SA}$ and $\mathbf{Q} = \mathbf{SB}$ are symmetric and $\mathbf{S}$ is positive definite. The matrix $\mathbf{S}$ is called the symmetrizer.

Lemma 3.1

There exists a matrix G such that the matrices $\mathbf{M} = \mathbf{GAG}^{-1}$ and $\mathbf{N} = \mathbf{GBG}^{-1}$ are symmetric.

Proof of lemma 3.1 can be seen in reference[3]. The basic idea of construction of G relies on diagonalizing the A matrix using the matrix formed by its eigenvectors and multiplying the transformed system by a diagonal matrix whose entries are unknown [8]. These entries are determined so that the transformed B matrix is symmetric. If T is the matrix formed by the eigenvectors of A, then $T^{-1}AT$ will be diagonal but not $T^{-1}BT$. Further we use a diagonal matrix $D = (\alpha, \beta, \gamma, \delta)$ and form

$$\mathbf{D^{-1}T^{-1}ATD \quad and \quad D^{-1}T^{-1}BTD}.$$

The first matrix will still be diagonal so that it is symmetric while the second one becomes symmetric for the choice of $\alpha = 1$, $\beta = \sqrt{2}$, $\gamma = 1$, and $\delta = 1$. With this choice of parameters we obtain

$$S = \begin{bmatrix} 1 & 0 & 0 & -\dfrac{1}{\gamma} \\ 0 & \dfrac{1}{2} & 0 & 0 \\ 0 & 0 & \dfrac{1}{2} & 0 \\ -\dfrac{1}{\gamma} & 0 & 0 & \dfrac{3}{2\gamma^2} \end{bmatrix}$$

$$P = \begin{bmatrix} 0 & 0 & 0 & 0 \\ 0 & 0 & 0 & \dfrac{1}{2\gamma} \\ 0 & 0 & 0 & 0 \\ 0 & \dfrac{1}{2\gamma} & 0 & 0 \end{bmatrix}$$

$$Q = \begin{bmatrix} 0 & 0 & 0 & 0 \\ 0 & 0 & 0 & 0 \\ 0 & 0 & 0 & \dfrac{1}{2\gamma} \\ 0 & 0 & \dfrac{1}{2\gamma} & 0 \end{bmatrix}$$

$$SC = \begin{bmatrix} 0 & 0 & -1+\dfrac{1}{\gamma} & 0 \\ 0 & 0 & 0 & 0 \\ \dfrac{1}{2\gamma} & 0 & 0 & -\dfrac{1}{2\gamma} \\ 0 & \dfrac{1}{2\gamma r} & \dfrac{1}{\gamma}-\dfrac{3}{2\gamma^2} & 0 \end{bmatrix} .$$

Returning to the proof of the theorem we now multiply (3.8) on the left by $\mathbf{u}^T$ to obtain

$$\mathbf{u}^T S \mathbf{u}_t + \mathbf{u}^T P \mathbf{u}_r + \mathbf{u}^T Q \mathbf{u}_z + \mathbf{u}^T (SC) \mathbf{u} = \mathbf{u}^T SF. \qquad (3.9)$$

Since the matrices S, P , and Q are symmetric, we can write (3.9) as

$$\frac{1}{2}(\mathbf{u}^T S \mathbf{u})_t + \frac{1}{2}(\mathbf{u}^T P \mathbf{u})_r + \frac{1}{2}(\mathbf{u}^T Q \mathbf{u})_z + \mathbf{u}^T SC \mathbf{u} = \mathbf{u}^T SF. \qquad (3.10)$$

Let us define a quantity $H(t)$ that measures the energy associated with the system (3.10):

$$H(t) = \int_\Omega (\mathbf{u}^T S \mathbf{u}) \, dx = 2\pi \int_0^H \int_0^L r(\mathbf{u}^T S \mathbf{u}) \, dr \, dz. \qquad (3.11)$$

Using (3.10) we obtain,

$$\frac{dH}{dt} = 2\pi \left[- \int_0^H \int_0^L r(\mathbf{u}^T P \mathbf{u})_r \, dr \, dz - \int_0^H \int_0^L r(\mathbf{u}^T Q \mathbf{u})_z \, dr \, dz \right.$$
$$\left. - 2\int_0^H \int_0^L r \, \mathbf{u}^T SC \mathbf{u} \, dr \, dz + 2\int_0^H \int_0^L r \mathbf{u}^T SF \, dr \, dz \right].$$

Applying the divergence theorem, it follows

$$\frac{dH}{dt} = 2\pi \left[-\int_{\Gamma_1} Lu^T Pu \; dz + \int_0^H \int_0^L u^T Pu \; dr \; dz - \int_{\Gamma_2} ru^T Qu \; dr \right.$$

$$+ \int_{\Gamma_4} ru^T Qu \; dr - 2\int_0^H \int_0^L ru^T(SC)u \; dr \; dz$$

$$\left. + \int_0^H \int_0^L u^T SFr \; dr \; dz \right]. \tag{3.12}$$

It is easy to see that,

$$-2 \int_0^H \int_0^L ru^T(SC - \frac{P}{2r})u \; dr \; dz \; \leq \; K \left[\int_0^H \int_0^L ru^T Su \; dr \; dz \right] \quad , \tag{3.13}$$

where

$$SC - \frac{P}{2r} = \begin{bmatrix} 0 & 0 & -1+\dfrac{1}{\gamma} & 0 \\[2mm] 0 & 0 & 0 & -\dfrac{1}{4\gamma r} \\[2mm] \dfrac{1}{2\gamma} & 0 & 0 & -\dfrac{1}{2}\gamma \\[2mm] 0 & \dfrac{1}{4\gamma r} & \dfrac{1}{\gamma}-\dfrac{3}{2\gamma^2} & 0 \end{bmatrix} \quad ,$$

and K is a positive constant.

Thus,

$$\frac{dH}{dt} \; \leq \; 2\pi \left[-\int_{\Gamma_1} Lu^T Pu \; dz - \int_{\Gamma_2} ru^T Qu \; dr + \int_{\Gamma_4} ru^T Qu \; dr \right]$$

$$+ 4\pi \int_0^H \int_0^L uTSFr \; dr \; dz + KH. \tag{3.14}$$

The boundary condition $w = 0$ on Γ_1 gives

$$\int_{\Gamma_4} ru^T Qu \; dr = 0.$$

Now boundary conditions on Γ_1 and Γ_2 yield

$$\int_{\Gamma_1} Lu^T Pu \; dz = \int_0^H L \; \frac{pu}{\gamma} \; dz \geq \; 0$$

$$\int_{\Gamma_2} ru^T Qu \; dr = \int_0^L r \; p \; \frac{w}{\gamma} \; dr \geq \; 0.$$

Then (3.14) takes the simple form

$$\frac{dH}{dt} \; \leq \; 4\pi \int_0^H \int_0^L u^T SFr \; dr \; dz + KH. \tag{3.15}$$

Moreover,

$$\int_0^H \int_0^L u^T SF \; dr \; dz = \int_0^H \int_0^L (Gu)^T (GF) r \; dr \; dz.$$

By the Schwartz inequality,

$$\left| (Gu)^T (GF) \right| \le \frac{\eta}{2} u^T S u + \frac{1}{2\eta} F^T S F \ .$$

Hence

$$\left| \int_0^H \int_0^L u^T S F r \ dr \ dz \right| \le \frac{\eta}{2} \int_0^H \int_0^L u^T S u r \ dr \ dz + \frac{1}{2\eta} \int_0^H \int_0^L F^T S F r \ dr \ dz$$

for all $\eta > 0$. Thus we obtain

$$\frac{dh}{dt} \le (\eta + K) H + \frac{2\pi}{\eta} \int_0^H \int_0^L F^T S F r \ dr \ dz$$

or

$$\frac{d}{dt} (e^{-(\eta+K)t} H) \le \frac{2\pi}{\eta} e^{-(\eta+K)t} \int_0^H \int_0^L F^T S F r \ dr \ dz \ . \tag{3.16}$$

Integrating with respect to t and using the initial condition $u = 0$ at $t = 0$ gives us

$$2\pi e^{-(\eta+K)\tau} \int_0^H \int_0^L u^T S u r \ dr \ dz \le \frac{2\pi}{\eta} \int_0^\tau \int_0^H \int_0^L e^{-(\eta+K)t} F^T S F r \ dr \ dz \ . \tag{3.17}$$

Finally, we integrate with respect to τ to obtain the required energy estimate

$$\int_0^T \|e^{-\eta t} u\|_0^2 \ dt \le \frac{CT}{\eta} \int_0^T \|e^{-\eta t} F\|_0^2 \ dt$$

where C is a constant independent of F, for all $\eta > K$.

4. Numerical Considerations and results

The numerical method used here is a straightforward explicit method, second order accurate in space and time, commonly known as MacCormacks scheme. A split form of this scheme has been used for numerical calculations. Recall that the system under consideration can be written in the form

$$u_t + A u_r + B u_z + C u = F. \tag{4.1}$$

We further write the system in the form

$$u_t + F_r + G_z = H, \tag{4.2}$$

where $H = F - Cu$. We decompose H into H_1 and H_2 so that equation (4.2) is split according to

$$u_t + F_r = H_1 \tag{4.3}$$

$$u_t + G_z = H_2 \ . \tag{4.4}$$

Let us denote the solution operators of (4.3) and (4.4) by $L_r(\Delta t)$ and $L_z(\Delta t)$. Thus the solution of equation (4.2) is advanced according to

$$u^{n+1} = L_r L_z u^n \ . \tag{4.5}$$

In the calculations reported here H_1 and H_2 are chosen as

$$H_1 = H_2 = \frac{1}{2}H = \frac{1}{2}\left[w - \frac{u}{r}, 0, \frac{p-\rho}{\gamma}, f + w - \frac{\gamma u}{r}\right]^T. \tag{4.6}$$

Corresponding flux quantities F and G are

$$F = \left[u, \frac{1}{\gamma}p, 0, \gamma u\right]^T \tag{4.7}$$

$$G = \left[w, 0, \frac{1}{\gamma}p, \gamma w\right]^T. \tag{4.8}$$

Note that quantities H_1 and H_2 have singular terms near the origin. They are handled as follows: at $r = 0$, $\frac{u}{r}$ is replaced by u_r using L'Hospital's rule. Thus at $r = 0$, F and H_1 are modified according to

$$F = \left[\frac{3}{2}u, \frac{1}{\gamma}p, 0, \frac{3}{2}\gamma u\right]^T \tag{4.9}$$

$$H = \left[w, 0, \frac{p-\rho}{\gamma}, f + w\right]^T. \tag{4.10}$$

Moreover, $u = 0$ on the axis; thus (4.9) takes the form $F = \left[0, \frac{1}{\gamma}p, 0, 0\right]^T$ on the axis. Absorbing boundary conditions (2.4) and (2.5) are applied on Γ_1 and Γ_2. Also characteristic extrapolations were applied on these boundaries. For examples, on Γ_1 the radiative boundary condition is $p - \gamma u = 0$, which is an incoming characteristic (set equal to zero). In each cycle we compute $p + \gamma u = T$, the out-going characteristics. Solving for p and u from these two relations, we obtain $p = \frac{T}{2}$ and $u = \frac{T}{2\gamma}$. Similar consideration was given on Γ_2.

Numerical computations were performed on a 41×21 grid (i.e., 41 point in the r direction and 21 in the z direction). Nondimensional lengths L and H were chosen to be 30 and 10 respectively. Higher resolution in the z direction was essential for the stability of the code. Δt was chosen sufficiently small to meet the stability criteria of the scheme.

Special consideration on the choice of the source was given as indicated below. The source was modelled according to

$$f(r,z,t) = \begin{cases} \dfrac{\cos t}{\Delta r \sqrt{\Delta z}} & (r,z) = 0 \\ 0 & (r,z) \neq 0 \end{cases} \tag{4.11}$$

which is in l_2 while having a property that is closely related to $\frac{\delta(r)}{r}\delta(z)\cos t$. Physically such a source corresponds to a point source which oscillates harmonically. Effectiveness of the code was verified by comparing a solution that is reported in Cole and Greifinger [1] for a point source both in space and time of the form

$$f(r,z,t) = \frac{\delta(r)}{r}\delta(z)\delta(t). \qquad (4.12)$$

This was modelled by an l_2 source for numerical purposes as

$$f(r,z,t) = \frac{1}{\Delta r\sqrt{\Delta z\Delta t}} \cdot \qquad (4.13)$$

An interesting case here occurs when the source takes the form (4.11). According to our estimate given by theorem (3.1), it is valid only for finite time. As time steadily grows the solution may become unbounded. Our computational results indicate such a phenomenon. Up to five periods (10π units) of time, the solution propagated through the radiation boundaries smoothly. Above that time the solution had a tendency to grow in the computational domain. We shall show this result up to ten periods of time.

All the results presented herein correspond to a source located at $r = 0$, $z = 0$ as indicated by (4.11). In figure (4.1) we show the time history of the pressure wave on the radiation boundary at the sixth grid point in the z direction. As we see from the figure, the solution starts from a state of rest and reaches a harmonic state. In particular the amplitude diminishes. For this case we have also plotted the time history of the wave at the same z level at four different locations of the computational domain: $r = 5$, $r = 10$, $r = 15$ and $r = 20$. The radiation boundary Γ_1 is at $r = 30$ (see figures (4.2) (a)-(d)).

The sound pressure level distribution is of interest from the physical point of view. This is illustrated in figure (4.3). In the absence of gravitational effects, the sound pressure level will be monotonically decreasing since the pressure decay is inversely proportional to the distance of observation. Clearly this is not the case as seen in figure (4.3). This is one of the features of the propagation of sound in the atmosphere. At certain regions sound may not be detected while at the same time, it is possible to detect the sound at a further distance from the source.

Figures (4.4) and (4.5) repeat the calculations of the above situation for ten periods of time. Figure (4.4) shows that roughly after seven periods of time, the solution begins to grow. Further increases in time lead to more growth in the solution. This occurs even with higher order corrections in radiation boundary conditions. Figure (4.5) illustrates the sound pressure level distribution in this situation. The phenomena for growth as well as nonlinear correction to the problem shall be considered in a later paper.

Acknowledgements:

Appendix

Derivation of the field equations

We shall begin with the statement of the fluid flow problem that governs the acoustic phenomena. If P^* is the ambient pressure and h is the scale height, then the nondimensional form of the Euler equations (the equations of continuity, balance of momentum, and energy) is

$$\frac{\partial \rho}{\partial t} + \text{div}(\rho q) = 0 \tag{A.1}$$

$$\frac{\partial q}{\partial t} + (q \cdot \nabla)q = -\frac{1}{\gamma \rho}\nabla \bar{p} - \frac{1}{\gamma}\hat{k} \tag{A.2}$$

$$\left[\frac{\partial}{\partial t} + q \cdot \nabla\right]\frac{\bar{p}}{\rho^\gamma} = \frac{1}{\rho^{\gamma-1}} \varepsilon f(x,y,z,t) . \tag{A.3}$$

Note that in equation (A.2) the forcing term $\frac{-1}{\gamma}\hat{k}$ ($\hat{k}$ is the unit vector in the z direction) arises due to the forcing term per unit mass $-g\hat{k}$ in the original variables which is due to gravity. In equation (A.3), f(x,y,z,t) dictates the space time dependency of the source, and ε measures the energy release per unit volume. For the case of an instantaneous energy release, ε is given by

$$\varepsilon = \frac{(\gamma - 1)Q_0}{h^3 P^*} \tag{A.4}$$

where Q_0 is the total energy released at time t = 0. The initial conditions are

$$\bar{p} = \rho = e^{-z}, \quad q = 0 \text{ at } t = 0, \tag{A.5}$$

which represent a calm atmosphere and exponentially decaying pressure and density.

The boundary condition at z = 0 is

$$q_z = 0, \tag{A.6}$$

which states that the vertical component of the flow is zero at z = 0.

The acoustic expansion is based on $\varepsilon \ll 1$ and represents the flow as small changes superimposed on the flow of the ambient state. We note that the ambient velocity is zero, but pressure and density have the form e^{-z}. Thus, the expansions are

$$q = \varepsilon u + \varepsilon^2 u_1 + \cdots \tag{A.7}$$

$$\overline{p} = e^{-z}\left[1 + \varepsilon p + \varepsilon^2 p_1 + \cdots\right] \tag{A.8}$$

$$\rho = e^{-z}\left[1 + \varepsilon \sigma + \varepsilon^2 \sigma_1 + \cdots\right] \tag{A.9}$$

where $u = (u, w)$ and $u_1 = (u_1, w_1)$. Quantities u, u_1 and w, w_1 are the r and z components of the acoustic velocities, respectively in cylindrical coordinates. We substitute expansions (A.7)-(A.9) into equations (A.1)-(A.3), initial conditions (A.5), and boundary conditions (A.6) and retain terms of order ε to obtain the field equations.

Time History of Pressure at the Right Boundary

Figure (4.1)

Pressure Wave at r=5
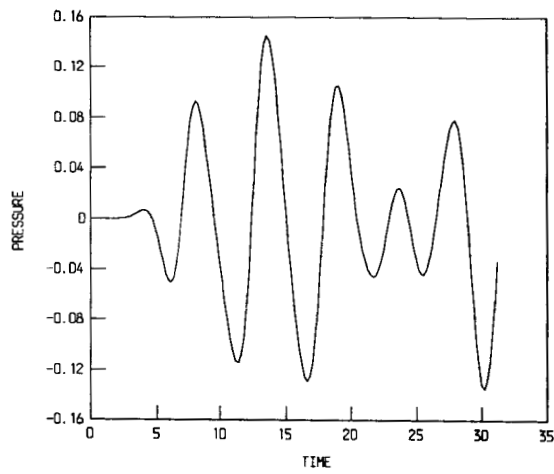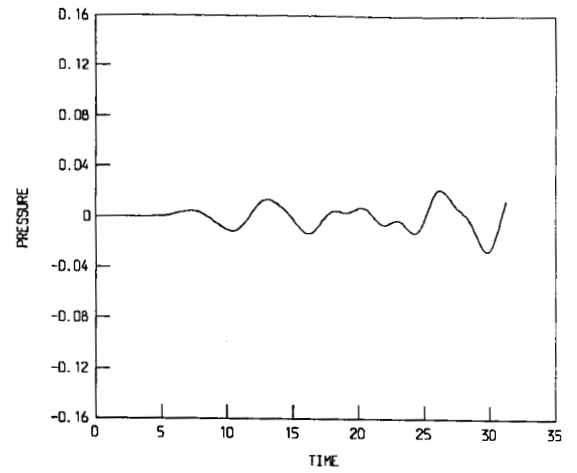
Figure (4.2a)

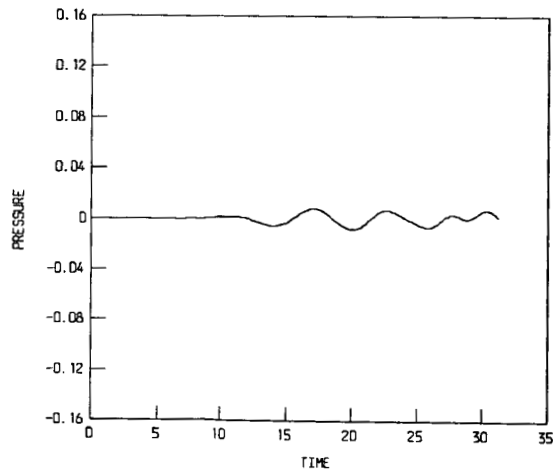Pressure Wave at r=10

Figure (4.2b)

Pressure Wave at r=15

Figure (4.2c)
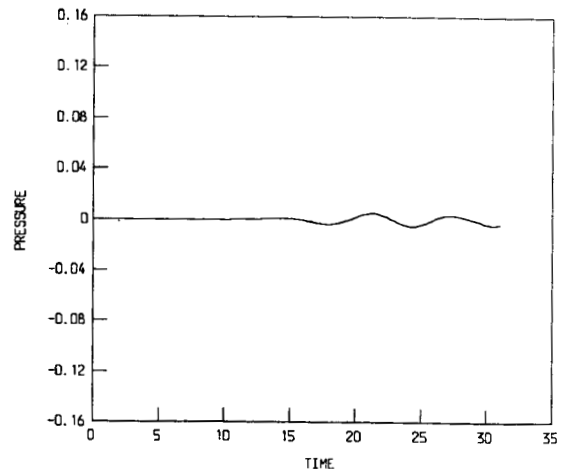
Pressure Wave at r=20

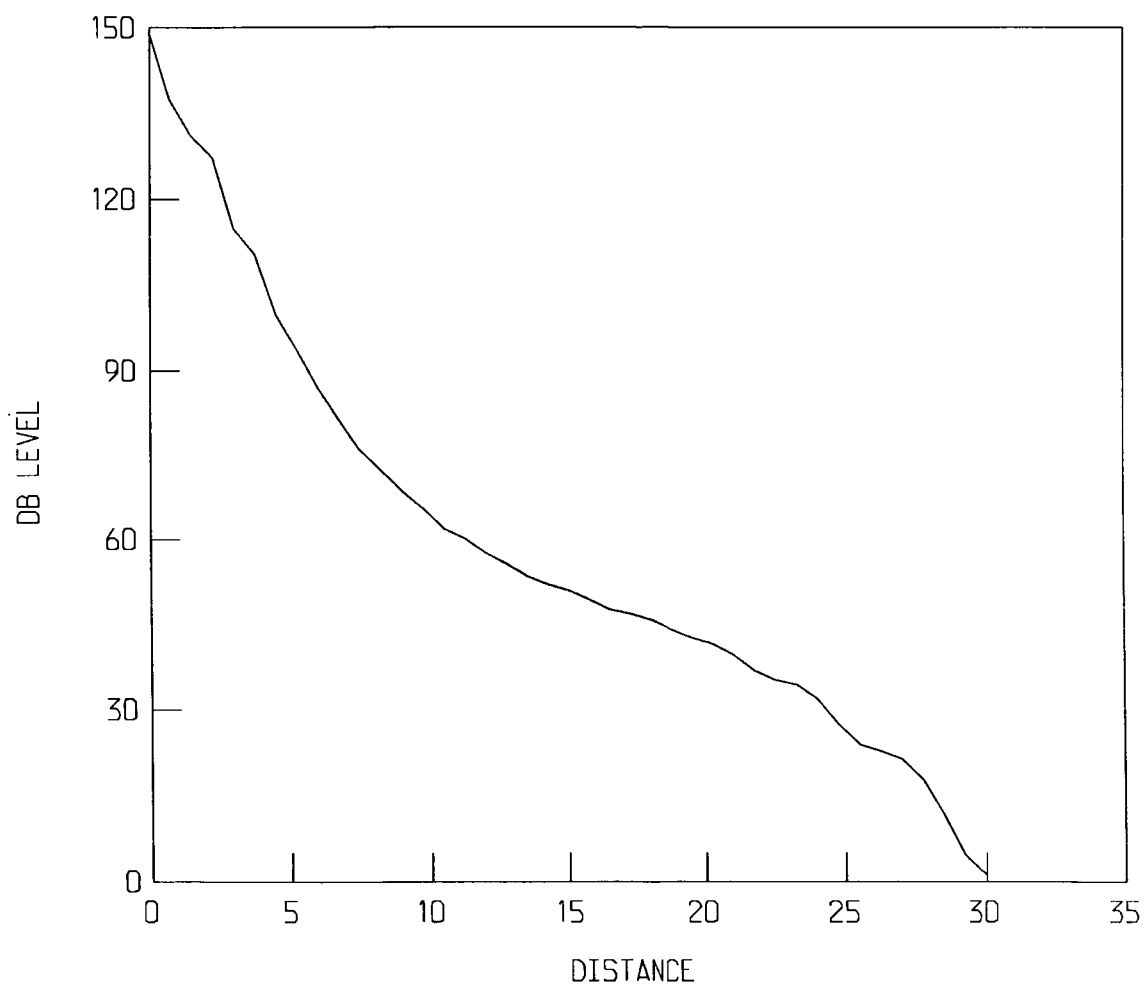Figure (4.2d)

Decibel Level Distribution

Figure (4.3)

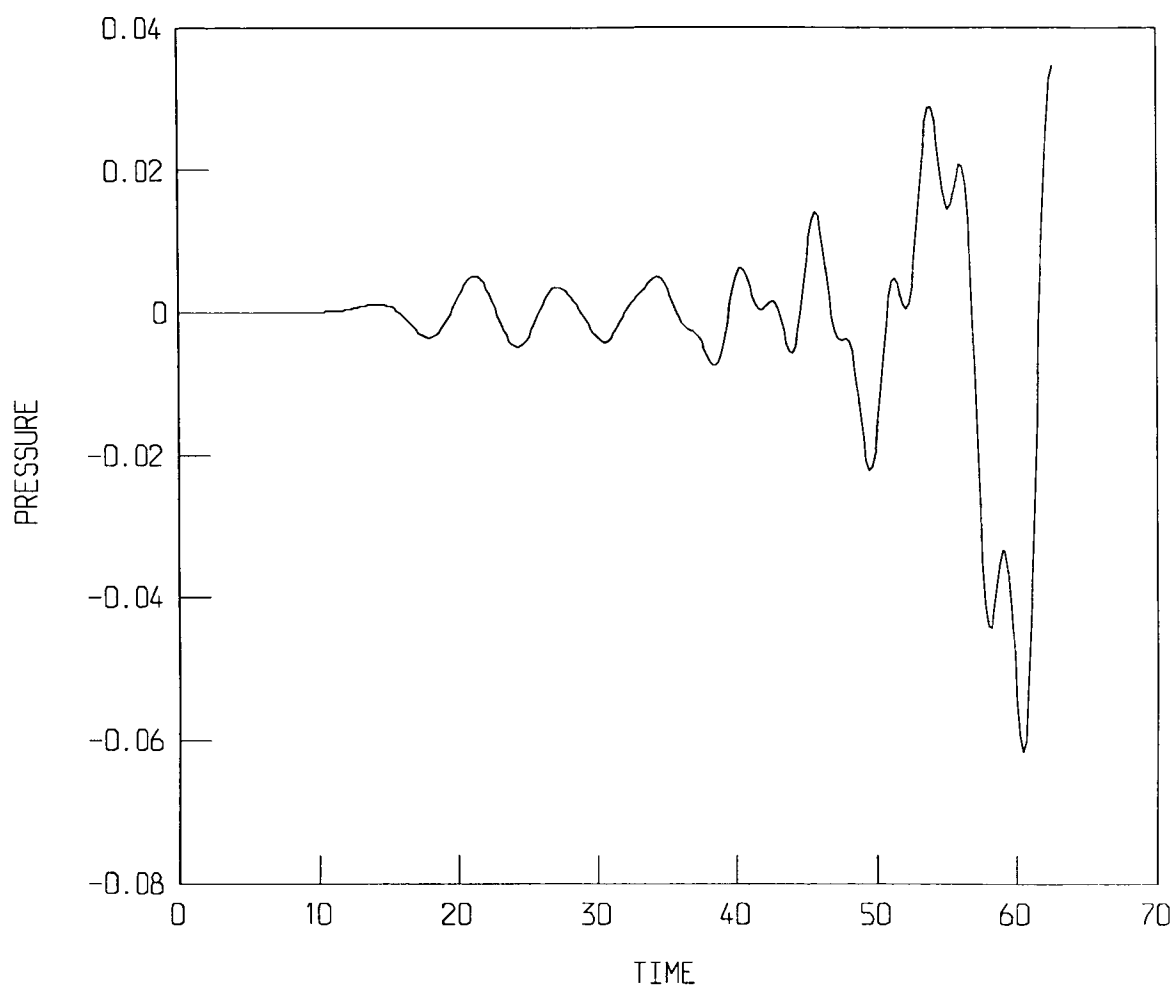Time History of Pressure at the Right Boundary
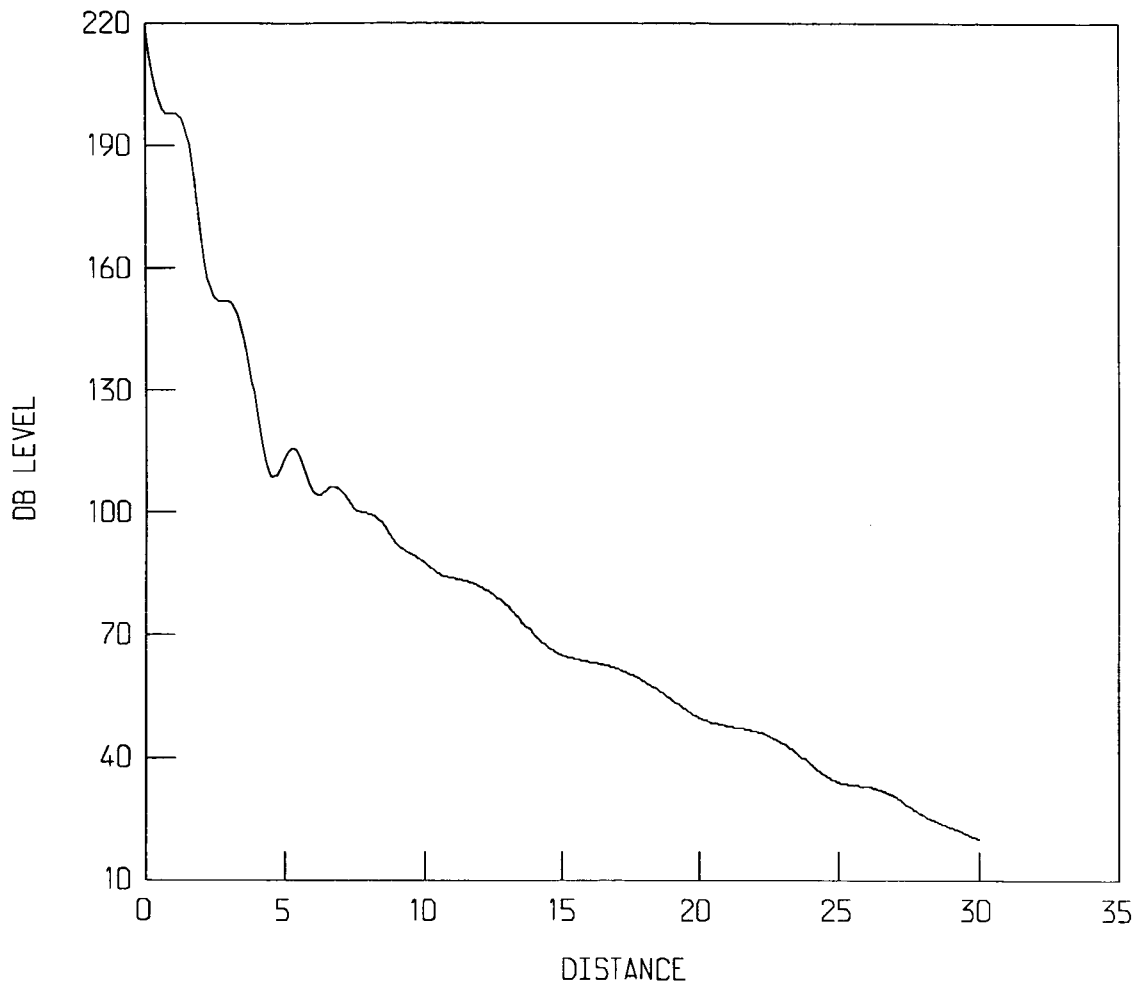
Figure (4.4)

Decibel Level Distribution

Figure (4.5)

References

[1] Cole, J.D. and C. Greifinger, "Acoustic Gravity Waves Produced by Energy Release," RAND Corp. Report RM-5738, 1968.

[2] Hariharan, S.I., "Nonlinear Acoustic Wave Propagation in Atmosphere," ICASE Report No. 86-10, 1986.

[3] Hariharan, S.I., "A Model Problem for Acoustic Wave Propagation in the Atmosphere," *Proceedings of the First IMACS Symposium on Computational Acoustics,* North Holland, Eds. D. Lee, R.L. Sternberg, and M.H. Schultz (in press).

[4] Hariharan, S.I. and H.C. Lester, "Acoustic Shocks in a Variable Area Duct Containing Near Sonic Flows," *J. Comp. Phys.,* Vol. 58, No. 1 (1985).

[5] Engquist, B. and A. Majda, "Absorbing Boundary Conditions for Acoustic and Elastic Wave Calculations," *Comm. Pure Appl. Math.,* Vol. 32, pp. 312-358, 1979.

[6] Bamberger, A., L. Halpern, P. Jolly, and B. Engquist, "The Paraxial Approximation for the Wave Equation: Some New Results," *Advances in Computer Methods for Partial Differential Equations - V,* (IMACS), Eds. R. Vichnevetsky and R.S. Stapleman (1984).

[7] Kreiss, H.O., "Initial Boundary Value Problems for Hyperbolic Systems," *Comm. Pure Appl. Math.,* Vol. 23, pp. 277-298, 1970.

[8] Abarbanel, S. and D. Gottlieb, "Optimal time splitting for two and three dimensional Navier-Stokes equations with mixed derivatives," *J. Comp. Phys.,* Vol. 41, No. 1 (May 1981), pp. 1-33.

1. Report No. NASA CR-178270 ICASE Report No. 87-19	2. Government Accession No.	3. Recipient's Catalog No.
4. Title and Subtitle ACOUSTIC GRAVITY WAVES: A COMPUTATIONAL APPROACH		5. Report Date March 1987
		6. Performing Organization Code
7. Author(s) S. I. Hariharan and P. K. Dutt		8. Performing Organization Report No. 87-19
9. Performing Organization Name and Address Institute for Computer Applications in Science and Engineering Mail Stop 132C, NASA Langley Research Center Hampton, VA 23665-5225		10. Work Unit No.
		11. Contract or Grant No. NAS1-18107
12. Sponsoring Agency Name and Address National Aeronautics and Space Administration Washington, D.C. 20546		13. Type of Report and Period Covered Contractor Report
		14. Sponsoring Agency Code 505-90-21-01

15. Supplementary Notes
Langley Technical Monitor: Submitted to Applied Numerical J. C. South   Mathematics Final Report

16. Abstract

This paper discusses numerical solutions of a hyperbolic initial boundary value problem that arises from acoustic wave propagation in the atmosphere. Field equations are derived from the atmospheric fluid flow governed by the Euler equations. The resulting original problem is nonlinear. A first order linearized version of the problem is used for computational purposes. The main difficulty in the problem as with any open boundary problem is in obtaining stable boundary conditions. Approximate boundary conditions are derived and shown to be stable. Numerical results are presented to verify the effectiveness of these boundary conditions.

17. Key Words (Suggested by Authors(s)) atmospheric acoustics, hyperbolic systems, well-posedness, finite differences	18. Distribution Statement 64 - Numerical Analysis 71 - Acoustics Unclassified - unlimited

19. Security Classif.(of this report) Unclassified	20. Security Classif.(of this page) Unclassified	21. No. of Pages 26	22. Price A03